Available on CMS information server **CMS NOTE 2001/008**

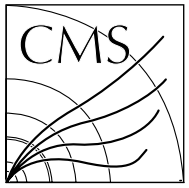

The Compact Muon Solenoid Experiment

CMS Note

Mailing address: CMS CERN, CH-1211 GENEVA 23, Switzerland

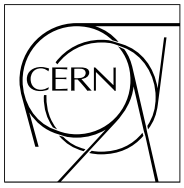

February 2001

High-mass dimuon and secondary J/ψ production at CMS as probes of medium-induced bottom quark energy loss in heavy ion collisions

I.P. Lokhtin and A.M. Snigirev

M.V. Lomonosov Moscow State University, D.V. Skobeltsyn Institute of Nuclear Physics, Moscow, Russia

Abstract

The capability of the CMS detector to observe the rescattering and energy loss of heavy quarks in the dense matter created in heavy ion collisions is discussed. We analyze the sensitivity of high-mass $\mu^+\mu^-$ pairs from $B\overline{B}$ semileptonic decays and secondary J/ψ's from single B decays to the medium-induced bottom quark energy loss.

1 Introduction

The significant progress in lattice QCD calculations, in particular, including dynamical quarks, strongly suggests that the deconfinement of hadronic matter and chiral symmetry restoration must happen at temperatures above $T_c \sim 200$ MeV [1]. Experimental studies of the properties of strongly interacting matter at high enough energy densities for a relatively long-lived quark-gluon plasma (QGP) to be formed is one of the goals of modern high energy physics (see, for example, reviews in Ref. [2, 3, 4, 5]). It is expected that the quark-hadron phase transition, which likely occurred during the first few microseconds of the evolution of the universe, can be attained in heavy-ion accelerators.

In recent years, a great deal of attention has been devoted to "hard" probes of the QGP including heavy quarkonia, hard hadrons, jets, and high mass dimuons which are not part of the thermalized system, thus carrying information about the early stages of the evolution. In particular, the predicted charmonium suppression by screening of bound $c\overline{c}$ pairs ("colour dipole") in a plasma [6] or dynamical dissociation by semi-hard deconfined gluons [7] is one of the most promising signals of QGP formation. A similar phenomenon has been observed in the most central Pb+Pb collisions at CERN-SPS [8]: the anomalously small J/ψ to Drell-Yan ratio, inconsistent with pre-resonance absorption in cold nuclear matter. Although the interpretation of this phenomenon as a result of QGP formation is plausible, alternative explanations such as rescattering with comoving hadrons can not be fully dismissed [9]. For the heavier $b\overline{b}$ bound states (the Υ family), a similar suppression effect in QGP is expected at the higher temperatures which can be attained in heavy ion collisions at the LHC.

Along with quarkonium suppression one process of interest is the passage of coloured jets through dense matter. Dijets are created at the very beginning of the collision process, $\lesssim 0.01$ fm/c, by the initial hard parton-parton scatterings. These hard partons pass through the dense matter formed by minijet production at longer time scales, ~ 0.1 fm/c, and interact strongly with the constituents of the medium. The inclusive cross section for hard jet production is negligible at the SPS but increases rapidly with the collision energy. Thus these jets will play an important role at RHIC (with Au+Au collisions at $\sqrt{s} = 200A$ GeV) and LHC (with Pb+Pb collisions at $\sqrt{s} = 5.5A$ TeV). The challenge is to determine the behaviour of coloured jets in dense matter [10] due to coherent medium-induced gluon radiation [11, 12, 13, 14, 15, 16] and collisional energy loss due to elastic rescatterings [17, 18, 19]. Since the jet rescattering intensity strongly increases with temperature, formation of a "hot" QGP at initial temperatures up to $T_0 \sim 1$ GeV at LHC [20] should result in much larger parton energy loss compared to "cold" nuclear matter or a hadronic gas.

The following signals of medium-induced energy loss have been identified as being observable [21] in heavy ion collisions using the CMS detector [22]:
1) The suppression of high-p_T jet pairs [23, 24] with a corresponding enhancement of the monojet-to-dijet ratio [25, 26]. Jets are produced in the initial scattering processes such as

$$gg \to gg\,, \quad qg \to qg\,, \quad qq \to qq\,, \quad gg \to q\overline{q}$$

where the $gg \to gg$ process is dominant.
2) The p_T-imbalance between a produced jet with a gauge boson in γ+jet [27] and Z+jet [28] production, e.g.

$$qg \to q\gamma\,, \qquad qg \to qZ.$$

The Z-boson is identified through its decays to muon pairs, $Z \to \mu^+\mu^-$.
3) The modification of the high mass dimuon spectra from semileptonic B and D meson decays due to bottom and charm quark energy loss [29, 30, 31]:

$$gg \to b\overline{b}\,(c\overline{c}) \to B\overline{B}\,(D\overline{D}) \to \mu^+\mu^- X.$$

In our previous work [32] we discussed the capability of the CMS detector to observe the energy loss of quark- and gluon initiated jets in Pb+Pb collisions using jet+jet, γ+jet and Z+jet production channels. The main goal of this paper is to analyze the sensitivity of both high-mass $\mu^+\mu^-$ pairs from $B\overline{B}$ semileptonic decays and secondary J/ψ's from single B decays to b-quark energy loss in CMS. Note that the ALICE experiment [33] will also study dilepton production in heavy ion collisions although with a different rapidity acceptance: $|\eta^\mu| < 2.4$ for CMS while $|\eta^e| < 0.9$ and $2.5 < |\eta^\mu| < 4$ for ALICE. We believe that dimuon production in combination with high-p_T jet production by gluon and light quark fragmentation can give important information about the medium-induced effects for both light and heavy partons in heavy ion collisions at the LHC.

The high-mass dimuon spectra in Pb+Pb collisions at LHC has already been estimated in the CMS acceptance [31] assuming a constant energy loss per unit length of $dE/dx = 1$ GeV/fm. In our paper we consider the dynamical

evolution of heavy quark energy loss and rescattering as a function of energy density in an expanding "hot" gluon-dominated plasma. We also investigate, for the first time, these effects on secondary J/ψ production from single B-meson decays.

2 Medium-induced gluon radiation from massive quarks

We first discuss the effects of the medium on gluon radiation from heavy quarks. We emphasize that the recent theoretical developments on medium-induced gluon radiation [13, 14] are valid in the coherent domain only in the ultrarelativistic limit of the quark momenta. Although some attempts have been made to calculate medium-induced heavy quark energy loss for quarks of mass M_q [34], a full description of the coherent radiation from a massive object still does not exist. There are two extreme limits for energy loss by gluon radiation. In the low p_T limit, $p_T \lesssim M_q$, medium-induced radiation should be suppressed by the mass, while the ultrarelativistic limit, $p_T \gg M_q$, corresponds to the radiation spectrum of massless quarks.

The approach developed in Ref. [34] is based on a factorization of the matrix elements into elastic scattering and gluon emission [35] where the multiplicity distribution of the radiated gluons can be written as

$$\frac{dN_g}{d\eta d^2q_T} = \frac{3\alpha_s}{\pi^2}\frac{l_T^2}{q_T^2(\vec{q_T}-\vec{l_T})^2}, \tag{1}$$

where $q=(q_0,\vec{q_T},q_3)$ and $l=(l_0,\vec{l_T},l_3)$ are the 4-momenta of the emitted and the exchanged gluon respectively and $\eta=(1/2)\ln\left[(q_0+q_3)/(q_0-q_3)\right]$ is the rapidity of emitted gluon relative to the initial quark momentum. It is valid in a limited q_T-region for small rapidities $\eta\sim 0$ and $l_T(q_0/E)\ll q_T$. The coherent LPM effect is taken into account simply by including a formation time restriction via a step function [12]. However, for light quarks, it leads to a different dependence of the radiative energy loss on the initial quark energy E than found in other, more recent works [13, 14].

In our case, the main contribution to high-mass dimuon and secondary J/ψ production is due to b-quarks with "intermediate" values of $p_T \gtrsim 5$ GeV/c, expected to be rather close to the incoherent regime. In order to estimate the sensitivity of the dimuon spectra to medium-induced effects, we consider two extreme cases: (i) the "minimum" effect with collisional energy loss only and (ii) the "maximum" effect with collisional and radiative energy loss in the incoherent limit of independent emissions without taking into account the LPM coherent suppression of radiation (i.e. $dE/dx\propto E$ and is independent of path length, L). In the latter scenario we use the Bethe-Heitler cross section obtained in relativistic kinematics and derive the medium-induced radiative energy loss per unit length [14] as the integral over the gluon radiation spectrum

$$\frac{dE}{dx} = E\rho\int\limits_0^{1-M_q/E} dy\frac{4\alpha_s C_3(y)(4-4y+2y^2)}{9\pi y\left[M_q^2y^2+m_g^2(1-y)\right]}, \tag{2}$$

$$C_3(y) = \frac{9\pi\alpha_s^2 C_{ab}}{4}\left[1+(1-y)^2-y^2\right]\ln\frac{2\left(\alpha_s^2\rho E y(1-y)\right)^{1/4}}{\mu_D},$$

where $m_g\sim 3T$ is the effective mass of the emitted gluon at temperature T, $y=q_0/E$ is the fraction of the initial quark energy carried by the emitted gluon, $\rho\propto T^3$ is the density of the medium and the Debye screening mass squared, $\mu_D^2=4\pi\alpha_s T^2(1+N_f/6)$, regularizes the integrated parton rescattering cross section.

3 Heavy quark rescattering in a dense QCD-medium

We have developed a Monte-Carlo simulation of the mean free path of heavy quarks ($M_b=5$ GeV and $M_c=1.5$ GeV) in an expanding QGP formed in the nuclear overlap zone in Pb+Pb collisions. The details of the geometrical model of hard quark production and the quark passage through dense matter can be found in our recent work [24]. In general, the intensity of rescattering and energy loss are sensitive to the initial conditions (energy density ε_0 and formation time τ_0) and space-time evolution of the medium, treated as a longitudinally expanding quark-gluon fluid. The partons are produced on a hyper-surface of equal proper times $\tau=\sqrt{t^2-z^2}$ [36].

If the mean free path of a hard parton is larger than the screening radius in the QCD-medium, $\lambda\gg\mu_D^{-1}$, the successive scatterings can be treated as independent [12]. The transverse distance between successive scatterings,

$\Delta x_i = (\tau_{i+1} - \tau_i)v_T = (\tau_{i+1} - \tau_i)p_T/E$, is generated according to the probability density

$$\frac{dP}{d(\Delta x_i)} = \frac{1}{\lambda(\tau_{i+1})} \exp\left(-\int_0^{\Delta x_i} \frac{ds}{\lambda(\tau_i + s)}\right) \tag{3}$$

where the inverse mean free path is $\lambda = 1/(\sigma\rho)$. The density of the medium $\rho(\tau)$ and the quark rescattering cross section $\sigma(\tau)$ are functions of proper time. Then the basic kinetic integral equation for the energy loss ΔE as a function of initial energy E and path length L has the form

$$\Delta E(L, E) = \int_0^L dx \frac{dP(x)}{dx} \lambda(x) \frac{dE(x, E)}{dx}\,, \tag{4}$$

$$\frac{dP(x)}{dx} = \frac{1}{\lambda(x)} \exp\left(-x/\lambda(x)\right),$$

where the current transverse coordinate of a quark, $x(\tau)$, is determined from $dx/d\tau = v_T$ with $x = \tau$ at v_T = 1.

The dominant contribution to the differential cross section $d\sigma/dt$ for scattering of a quark with energy E and momentum $p = \sqrt{E^2 - M_q^2}$ off the "thermal" partons with energy (or effective mass) $m_0(\tau) \sim 3T(\tau) \ll E$ at temperature T can be written as [12, 34]

$$\frac{d\sigma_{ab}}{dt} \cong C_{ab} \frac{2\pi\alpha_s^2(t)}{t^2} \frac{E^2}{p^2} \tag{5}$$

where $C_{ab} = 9/4$, 1, and 4/9 for gg, gq and qq scatterings respectively. The strong coupling constant is

$$\alpha_s(t) = \frac{12\pi}{(33 - 2N_f)\ln\left(t/\Lambda_{\rm QCD}^2\right)} \tag{6}$$

for N_f active quark flavours and QCD scale parameter $\Lambda_{\rm QCD}$ on the order of the critical temperature, $\Lambda_{\rm QCD} \simeq T_c$. The integrated parton scattering cross section is regularized by the Debye screening mass squared μ_D^2:

$$\sigma_{ab}(\tau) = \int_{\mu_D^2}^{t_{\rm max}} dt \frac{d\sigma_{ab}}{dt} \tag{7}$$

where $t_{\rm max} = [s - (M_q + m_0)^2][s - (M_q - m_0)^2]/s$ and $s = 2m_0E + m_0^2 + M_q^2$.

In the i-th rescattering with squared momentum transfer t_i and effective mass m_{0i}, the quark loses total energy Δe_i and transverse energy Δe_i^T as well as getting a transverse momentum kick $\Delta\tilde{\mathbf{k}}_{ti}$ relative to the initial momentum $\mathbf{p}$. It is straightforward to evaluate Δe_i, Δe_i^T and $\Delta\tilde{\mathbf{k}}_{ti}$ at quark longitudinal rapidity Y:

$$\Delta e_i = \frac{t_i}{2m_{0i}}, \tag{8}$$

$$\Delta e_i^T = \frac{\Delta e_i}{\cosh Y} - \Delta\tilde{k}_{ti} \tanh Y, \tag{9}$$

$$\Delta\tilde{k}_{ti} = \sqrt{\left(E - \frac{t_i}{2m_{0i}}\right)^2 - \left(p - \frac{E}{p}\frac{t_i}{2m_{0i}} - \frac{t_i}{2p}\right)^2 - M_q^2}, \tag{10}$$

$$\Delta\tilde{\mathbf{k}}_{ti} = \Delta\tilde{k}_{ti}(\mathbf{e_1}\cos\phi + \mathbf{e_2}\sin\phi), \tag{11}$$

where the unit vectors $(\mathbf{e_1} \perp \mathbf{e_2})$ specify the plane orthogonal to the quark momenta $\mathbf{p}$ and the azimuthal angle ϕ is distributed uniformly. The medium-induced radiative energy loss is calculated with Eq. (2) without modification of the longitudinal rapidity.

In our calculations, we use the Bjorken scaling solution [36] for the space-time evolution of the energy density, temperature and density of the plasma:

$$\varepsilon(\tau)\tau^{4/3} = \varepsilon_0\tau_0^{4/3}, \tag{12}$$

$$T(\tau)\tau^{1/3} = T_0\tau_0^{1/3}, \tag{13}$$

$$\rho(\tau)\tau = \rho_0\tau_0. \tag{14}$$

To be specific, we use the initial conditions for a gluon-dominated plasma expected for central Pb+Pb collisions at LHC [20]: $\tau_0 \simeq 0.1$ fm/c, $T_0 \simeq 1$ GeV, $N_f \approx 0$, $\rho_g \approx 1.95T^3$. It is interesting that the initial energy density, ε_0, in the dense zone depends on b very slightly, $\delta\varepsilon_0/\varepsilon_0 \lesssim 10\%$, up to $b \sim R_A$ and decreases rapidly for $b \gtrsim R_A$ [24]. On the other hand, the proper time of a jet to escape the dense zone averaged over all possible jet production vertices, $\langle\tau_L\rangle$, is found to decrease almost linearly with increasing impact parameter. This means that for impact parameters $b < R_A$, where $\approx 60\%$ of the heavy quark pairs are produced [21], the difference in rescattering intensity and the corresponding energy loss is determined mainly by the different path lengths rather than the initial energy density.

The simulation of quark rescattering is halted if one of the following three conditions is fulfilled:
1) A quark escapes from the dense zone, i.e. its path length becomes greater than the effective transverse spread of the matter from the production vertex to the escape point. The details of the geometrical calculations of these quantities at a given impact parameter can be found in Ref. [24].
2) The plasma cools down to $T_c = 200$ MeV. We thus neglect possible additional small contributions to the total energy loss due to re-interactions in the hadron gas.
3) A quark loses so much energy that its transverse momentum p_T drops below the average transverse momentum of the "thermal" constituents of the medium. In this case, such a quark is considered to be "thermalized" and its momentum in the rest frame of the fluid is generated from the random "thermal" distribution, $dN/d^3p \propto \exp(-E/T)$, boosted to the center-of-mass of the nucleus-nucleus collision [30, 31].

4 High-mass dimuon production in CMS

Let us first consider dimuon production in the high invariant mass region, $20 < M_{\mu^+\mu^-} < 50$ GeV/c^2, where

$$M_{\mu^+\mu^-} = \sqrt{(E_{\mu^+} + E_{\mu^-})^2 - (\mathbf{p}_{\mu^+} + \mathbf{p}_{\mu^-})^2}.$$

One of the main dimuon sources in this "resonance-free" mass region is the semileptonic decays of open bottom and charm mesons [37]. Heavy quark pairs are produced at the very beginning of the nuclear collisions by hard gluon-gluon scatterings and propagate through the dense medium. They finally form B and D mesons by "capturing" u, d or s quarks during the hadronization stage. These mesons will decay with the average meson lifetimes $c\tau_{B^\pm} = 495$ μm, $c\tau_{B^0} = 496$ μm, $c\tau_{D^\pm} = 315$ μm and $c\tau_{D^0} = 124$ μm. We note that $\approx 20\%$ of B mesons and $\approx 12\%$ of D mesons decay to muons. About half of the muons from B decays are produced through an intermediate D [38] and contribute to the softer part of the p_T-spectrum. There is also dimuon production from single B decays: $B \to \overline{D}\mu^+X \to \mu^+\mu^-Y$. The branching ratio for this channel is comparable to the yield from $b\overline{b}$ pair decay. However the muon pairs from single B's are concentrated in the low-mass region, $M_{\mu^+\mu^-} < M_B = 5.3$ GeV/c^2, below our interest here.

Note that at LHC energies, there can be a significant contribution to heavy flavour production from gluon splittings, $g \to Q\overline{Q}$, in initial- or final-state shower evolution [39]. However, although the probability for a high-p_T event to contain at least one $b\overline{b}$ or $c\overline{c}$ pair is fairly large, most of these quarks are carrying a small fraction of the total transverse momentum of the jet and dimuons produced in such a way are expected to be concentrated in the low invariant mass region.

The main correlated background is Drell-Yan production, $q\overline{q} \to \mu^+\mu^-$. The uncorrelated part of the dimuon background, random decays of pions and kaons and muon pairs of mixed origin, is comparable with the signal from $b\overline{b}$-decays [37] but these random decays also appear in the like-sign dimuon mass spectra. Thus such background can be estimated from the $\mu^+\mu^+$ and $\mu^-\mu^-$ event samples as [40]

$$\frac{dN^{\rm uncor}_{\mu^+\mu^-}}{dM} = 2\sqrt{\frac{dN_{\mu^+\mu^+}}{dM}\frac{dN_{\mu^-\mu^-}}{dM}}. \qquad (15)$$

and subtracted from the total $\mu^+\mu^-$ distribution.

The cross sections, $\sigma^{Q\overline{Q}}_{NN}$, for heavy quark production in NN collisions at $\sqrt{s} = 5.5$ TeV, the initial $Q\overline{Q}$ momentum spectra, and the B and D meson fragmentation have all been obtained using PYTHIA5.7 [41] with the default CTEQ2L parton distribution functions and including initial and final state radiation in vacuum which effectively simulates higher-order contributions to heavy quark production. The corresponding Pb+Pb cross section is obtained by multiplying $\sigma^{Q\overline{Q}}_{NN}$ by the number of binary nucleon-nucleon sub-collisions. The initial distribution

of $Q\overline{Q}$ pairs over impact parameter b can be written as [32, 42]

$$\frac{d^2\sigma^0_{Q\overline{Q}}}{d^2b}(b,\sqrt{s}) = T_{AA}(b)\sigma^{Q\overline{Q}}_{NN}(\sqrt{s})\frac{d^2\sigma^{AA}_{\rm in}}{d^2b}(b,\sqrt{s}) \tag{16}$$

where the differential inelastic AA cross section is

$$\frac{d^2\sigma^{AA}_{\rm in}}{d^2b}(b,\sqrt{s}) = \left[1-\left(1-\frac{1}{A^2}T_{AA}(b)\sigma^{\rm in}_{NN}(\sqrt{s})\right)^{A^2}\right] \tag{17}$$

and the total inelastic non-diffractive nucleon-nucleon cross section is $\sigma^{\rm in}_{NN} \simeq 60$ mb at $\sqrt{s} = 5.5$ TeV. The standard Wood-Saxon nuclear overlap function is $T_{AA}(b) = \int d^2s T_A(s)T_A(|\mathbf{b}-\mathbf{s}|)$ where $T_A(s) = A\int dz\rho_A(s,z)$ is the nuclear thickness function with nucleon density distributions $\rho_A(s,z)$ [43].

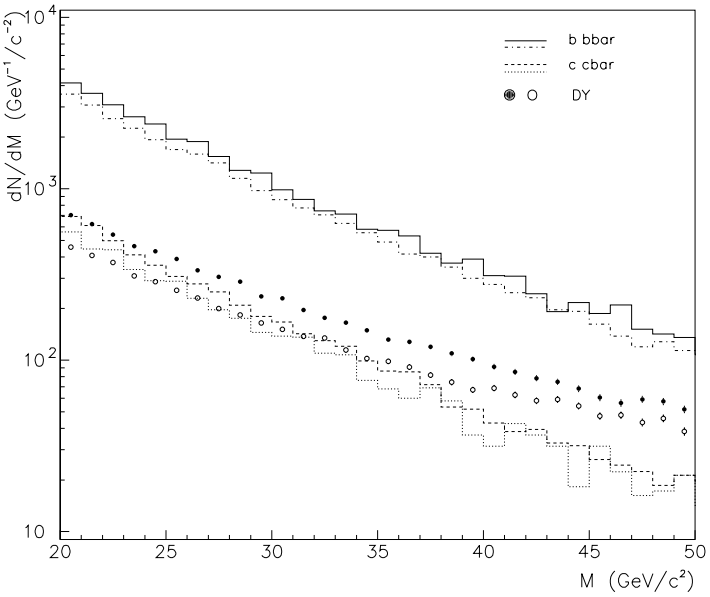

Figure 1: The initial invariant mass distribution of $\mu^+\mu^-$ pairs from correlated sources with $p_T^\mu > 5$ GeV/c and $|\eta^\mu| < 2.4$. The results are for $b\overline{b}$ (solid and dot-dashed histograms – without and with nuclear shadowing respectively), $c\overline{c}$ (dashed and dotted histograms), and Drell-Yan production (closed and open circles.)

We also take into account the modification of the nucleon structure functions due to the initial state nuclear interactions such as gluon depletion, nuclear shadowing, using the phenomenological parameterization of Eskola et al. [44]. Figure 1 shows the initial $\mu^+\mu^-$ invariant mass spectra from correlated $b\overline{b}$, $c\overline{c}$ and Drell-Yan production in the CMS acceptance, $p_T^\mu > 5$ GeV/c and $|\eta^\mu| < 2.4$. The upper and lower histograms for each contribution show the results without and with nuclear shadowing respectively. In this kinematical region the influence of nuclear shadowing on heavy quarks is relatively small, giving an $\approx 15\%$ reduction in the open bottom and charm decays. Drell-Yan production is somewhat more affected, with an $\approx 25\%$ reduction, because quark shadowing is stronger than gluon shadowing at low x in the EKS model [44]. The total impact-parameter integrated rates are normalized to the expected number of Pb+Pb events during a two week LHC run, $R = 1.2\times10^6$ s, assuming luminosity $L = 10^{27}$ cm^{-2}s^{-1} [22] to that

$$N(\mu^+\mu^-) = R\sigma^{\mu^+\mu^-}_{AA}\,L\ .$$

We see that the $b\overline{b} \to \mu^+\mu^-$ rates are greater than those from the other sources by a factor of at least 5. Thus we only consider dimuons from $b\overline{b}$ decays in the remainder of the discussion. Moreover, the medium-induced charm quark energy loss can be significantly larger than the b-quark loss due to the mass difference, resulting in an additional suppression of the $c\overline{c} \to \mu^+\mu^-$ yield.

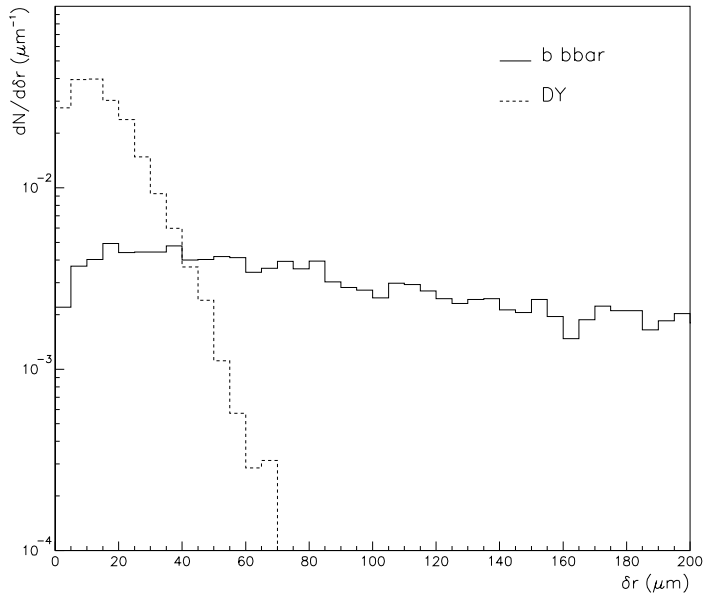

Figure 2: Distribution of $\mu^+\mu^-$ pairs from $b\overline{b}$ decays (solid histogram) and from Drell-Yan production (dashed histogram) as a function of δr.

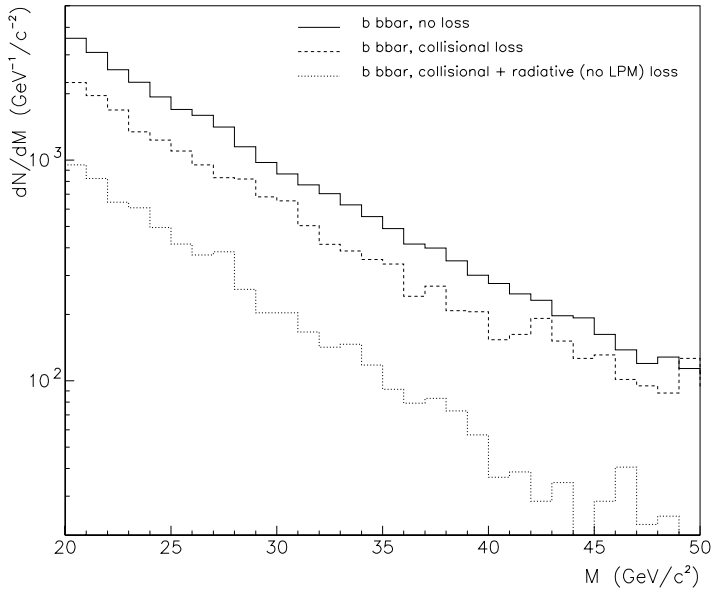

Figure 3: Invariant mass distribution of $\mu^+\mu^-$ pairs from $b\overline{b}$ decays with $p_T^\mu > 5$ GeV/c and $|\eta^\mu| < 2.4$ for various scenarios: without energy loss (solid histogram), with collisional loss only (dashed histogram), with collisional and radiative loss in incoherent limit (dotted histogram). Nuclear shadowing has been included.

Drell-Yan pairs are unaffected by medium-induced final state interactions. These dimuons are directly from the primary nuclear interaction vertex while the dimuons from B and D meson decays appear at secondary vertices some distance from the primary vertex. The path length between the primary vertex and secondary vertices are determined by the lifetime and γ-factor of the mesons. We have found that a good way to distinguish the dimuons from B mesons and those escaping from the primary vertex may be the transverse distance between the intersection points with the beam line for both tracks, δr. If $P_{\rm min}$ is defined as a track point with minimal distance to the beam axis, z, then δr is the distance in the $x-y$ plane between points $P^1_{\rm min}$ and $P^2_{\rm min}$ belonging different muon tracks. Figure 2 shows the distribution of muon pairs from $b\overline{b}$ decays and Drell-Yan production as a function of δr. We estimate the accuracy of the track position determination to be $\sigma_x = \sigma_y \sim 10$ μm and $\sigma_z \sim 100$ μm while the accuracy of the nuclear interaction point determination to be $\sigma_x = \sigma_y \sim \sigma_z \sim 20$ μm for the CMS tracking system [45]. We find that for a such simple simulation of the tracker resolution the cut $\delta r > 50$ μm suppresses the Drell-Yan rate by up to two orders of magnitude at the price of a 30% signal reduction. Of course, in order to be more conclusive, a full GEANT-based simulation including the real CMS geometry and dimuon reconstruction algorithm is needed [45].

Figure 3 presents the $\mu^+\mu^-$ invariant mass spectra from $b\overline{b}$ decays without and with the medium-induced b-quark energy loss described in sections 2 and 3, including nuclear shadowing. The initial dimuon rate in the mass range $20 < M_{\mu^+\mu^-} < 50$ GeV/c^2 is 2.8×10^4 events per two week run without energy loss or shadowing. The rate can be reduced by factor of $1.6 - 4$ due to rescattering and b-quark energy loss in the QGP. Note that the rate integrated over all phase space is always conserved: the suppression in the rate appears only when kinematic cuts are specified. The dimuon suppression due to collisional loss is more pronounced at relatively lower invariant masses since the collisional energy loss is almost independent of the initial quark energy. The relative contribution of medium-induced gluon radiation to total energy loss grows with increasing $M_{\mu^+\mu^-}$ because the radiative energy loss grows with increasing initial energy, $\propto E$ in the incoherent limit used in our calculations, and thus contributes to the whole high-mass dimuon range, especially in the large invariant mass domain. The loss increases for high momentum quarks which contribute to the larger dimuon masses.

To conclude this section, we note that there are theoretical uncertainties in the bottom and charm production cross sections in nucleon-nucleon collisions at LHC energies which affect the quark production rates without any loss effects. The absolute dimuon rates depend on the parton distribution functions, the heavy quark mass, the B-meson fragmentation scheme, next-to-leading order corrections, etc. Another possible contribution to the b quark cross section could be light gluinos decaying into b squarks [46], as proposed to explain the apparent deficit in the B cross section at the Tevatron. It is therefore desirable that high mass dimuon measurements in pp or dd collisions are made at the same or similar energy per nucleon as in the heavy ion runs.

5 Dimuons from $B \to J/\psi$ in CMS

We now consider another process which can also carry information about medium-induced rescattering and b-quark energy loss: secondary J/ψ production. The branching ratio $B \to J/\psi X$ is 1.15%. The J/ψ's subsequently decay to dimuons with a 5.9% branching ratio [38] so that e.g.

$$gg \to b\overline{b} \to B\overline{B}\, X \to J/\psi\, Y \to \mu^+\mu^- Y.$$

Figure 4 shows the transverse momentum and pseudo-rapidity distributions of secondary J/ψ decays for the same nuclear shadowing and energy loss scenarios described in the previous section. The total rates are again normalized to the expected number of events in a two week Pb+Pb run. We expect 1.3×10^4 dimuons from secondary J/ψ's at $M_{\mu^+\mu^-} = M_{J/\psi} = 3.1$ GeV/c^2. Including nuclear shadowing reduces this J/ψ yield by $\sim 25\%$ while the final state rescattering and energy loss by b-quarks can further reduce the J/ψ rates by a factor of $1.3 - 2.2$ in the CMS acceptance.

We see that the influence of nuclear effects on secondary J/ψ production and high-mass dimuon rates are quite different. The 25% decrease of the secondary J/ψ rate by nuclear shadowing is comparable to the $\sim 30 - 50\%$ effect of medium-induced final state interactions. On the other hand, the high-mass dimuon rates are reduced by up to a factor of 4 due to energy loss, much larger than the 15% nuclear shadowing correction. The increased sensitivity to nuclear shadowing is due to the different x and Q^2 regions probed. The different influence of energy loss on secondary J/ψ and high-mass dimuons is because secondary J/ψ's come from the decay of a single b quark instead of a $b\overline{b}$ pair and there is a non-negligible probability that the energy lost by one quark is small. Thus a comparison between high-mass dimuon and secondary J/ψ production could clarify the nature of energy loss.

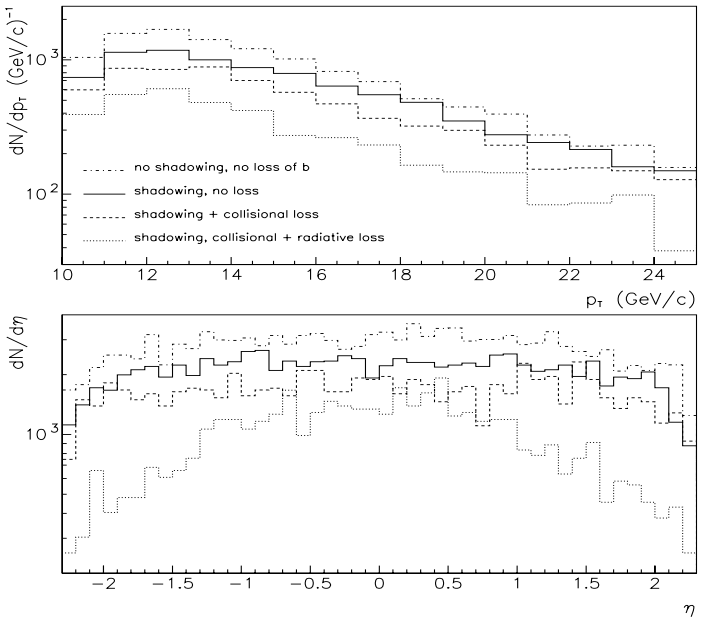

Figure 4: Transverse momentum and pseudo-rapidity distributions of secondary J/ψ decays with $p_T^\mu > 5$ GeV$/c$ and $|\eta^\mu| < 2.4$ for various scenarios: without nuclear shadowing and energy loss (dash-dotted histograms), with shadowing and without loss (solid histogram), with shadowing and collisional loss (dashed histogram) and with shadowing, collisional and radiative loss in the incoherent limit (dotted histogram).

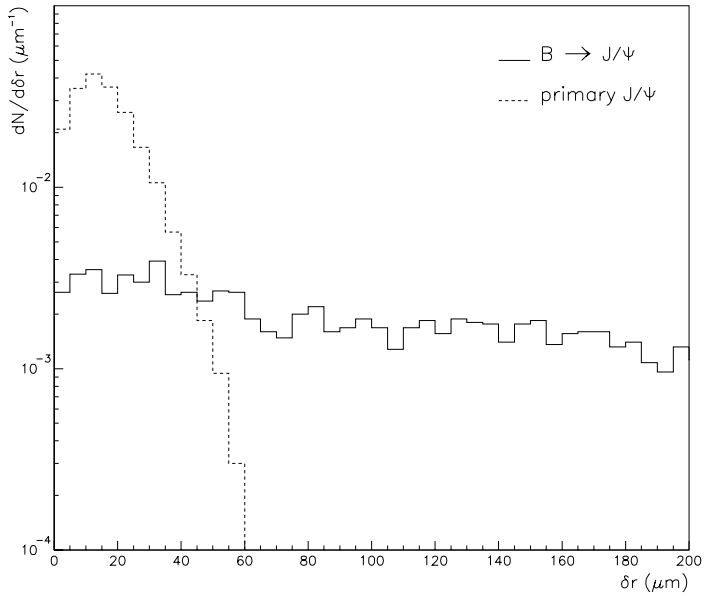

Figure 5: Distribution of $\mu^+\mu^-$ pairs from secondary (solid histogram) and primary (dashed histogram) J/ψ decays as a function of δr.

We note that about 5000 primary J/ψ's are expected to be initially produced by gluon-gluon fusion. The final primary J/ψ rate is rather uncertain: on one hand, it should be suppressed due to colour screening [6] and/or dynamical dissociation in a QGP [7]; on the other hand, "thermal" models predict some additional yield of J/ψ's from a QGP, see, e.g. Refs. [9, 47] and references therein. Other models suggest thatJ/ψ's can be regenerated in the hadron phase by $D\overline{D}$ interactions [48, 49]. Note that we call all these J/ψ's "primary" in the sense that they are from the primary nuclear interaction vertex. Although they could be produced late in the collision, either after thermalization or in the hadronization stages, the time scale of their formation is much less than the formation time of secondary J/ψ's from B meson decays. Thus it is necessary to distinguish secondary from primary J/ψ's. As in the case of separating dimuons from Drell-Yan production and $b\overline{b}$ decays, primary J/ψ's produced at the nuclear interaction point can be rejected using tracker information on the secondary vertex position. Figure 5 shows the δr-distribution of muon pairs from primary and secondary J/ψ's for the same conditions as in Fig. 2. We see that results in Figs. 2 and 5 are very similar. In addition, primary J/ψ's have a softer dimuon p_T spectrum than secondary J/ψ's and the primary J/ψ contribution disappears rapidly with increasing p_T.

6 Conclusions

To summarize, we have analyzed the sensitivity of spectra of high-mass $\mu^+\mu^-$ pairs from $b\overline{b}$ decays and dimuons from secondary J/ψ's to medium-induced bottom quark energy loss in Pb+Pb collisions at LHC in the CMS detector. Since a complete description of coherent radiation by massive quarks is still lacking, the dimuon spectra were calculated for two extreme cases: with collisional loss only, the "minimum" effect, and with collisional and radiative loss estimated in the incoherent limit, the "maximum" effect.

We have found that medium-induced parton rescattering and energy loss can reduce the dimuon rate in the invariant mass range $20 < M_{\mu^+\mu^-} < 50$ GeV/c^2 by a factor from 1.5 to 4 while nuclear shadowing is only of order of 15% in our kinematical region. The relative contribution of radiative energy loss to the total dimuon suppression grows with increasing invariant mass and p_T due to the stronger energy dependence of radiative loss relative to collisional loss.

Since secondary J/ψ production reflects the medium-induced energy loss of only one b-quark, the corresponding suppression by a factor of $1.3 - 2$ is less than for $b\overline{b}$ decays. On the other hand, the influence of nuclear shadowing on the relatively low invariant mass region, $M_{\mu^+\mu^-} \sim M_{J/\psi}$, seems to be non-negligible. We suggest that comparing high-mass dimuons with secondary J/ψ production would help clarify the nature of this phenomenon.

The recognition of high-mass dimuons from $b\overline{b}$ decays relative to Drell-Yan pairs, as well as the recognition of secondary compared to primary J/ψ's, could be performed using tracker information on the secondary vertex position.

We conclude that the dimuon spectra will be sensitive to final state rescattering and energy loss of bottom quarks in dense matter. However, there are still theoretical uncertainties in the initial production of heavy flavours in nucleon-nucleon collisions at LHC energies. Thus measurements in pp or dd collisions at the same or similar energies per nucleon as in the heavy ion runs are required.

Acknowledgments

It is a pleasure to thank D. Denegri for valuable suggestions and R. Vogt for important comments on this work. Discussions with M. Bedjidian, E. Boos, O.L. Kodolova, N.A. Kruglov, R. Kvatadze, A.N. Nikitenko, L.I. Sarycheva, S.V. Shmatov and U. Wiedemann are gratefully acknowledged.

References

[1] J. Engels et al., Phys. Lett. B396, 210 (1997); E. Laermann, Phys. Part. Nucl. 30, 304 (1999)

[2] H. Satz, Phys. Rep. 88, 349 (1982)

[3] J.W. Harris and B. Müller, Ann. Rev. Nucl. Part. Sci. 46, 71 (1996)

[4] I.P. Lokhtin, L.I. Sarycheva and A.M. Snigirev, Phys. Part. Nucl. 30, 279 (1999)

[5] S.A. Bass, M. Gyulassy, H. Stöcker and W. Greiner, J. Phys. G25, R1 (1999)

[6] T. Matsui and H. Satz, Phys. Lett. B178, 416 (1986)

[7] D. Kharzeev and H. Satz, Phys. Lett. B334, 155 (1994)

[8] M.C. Abreu et al. (NA50 Coll.), Phys. Lett. B410, 337 (1997); Phys. Lett. B450, 456 (1999)

[9] R. Vogt, Phys. Rep. 310, 197 (1999)

[10] R. Baier, D. Schiff and B.G.Zakharov, Annual Rev. Nucl. Part. Sci. 50, 37 (2000)

[11] M.G. Ryskin, Sov. J. Nucl. Phys. 52, 139 (1990)

[12] M. Gyulassy and X.-N. Wang, Nucl. Phys. B420, 583 (1994) 583; M. Gyulassy, M. Plümer, and X.-N. Wang, Phys. Rev. D51, 3436 (1995)

[13] R. Baier et al., Phys. Lett B345, 277 (1995); Nucl. Phys. B483, 291 (1997); Nucl. Phys. B531, 403 (1998); Phys. Rev. C58, 1706 (1998)

[14] B.G. Zakharov, JETP Lett. 63, 953 (1996); JETP Lett. 64, 781 (1996); JETP Lett. 65, 615 (1997); Phys. At. Nucl. 61, 838 (1998)

[15] U. Wiedemann and M. Gyulassy, Nucl. Phys. B560, 345 (1999); U. Wiedemann, Nucl. Phys. B588, 303 (2000); hep-ph/0008241

[16] M. Gyulassy, P. Levai and I. Vitev, Nucl. Phys. B 594, 371 (2001)

[17] J.D. Bjorken, Fermilab preprint 82/29-THY, 1982

[18] S. Mrówczyński, Phys. Lett. B269, 383 (1991); M. Thoma, Phys. Lett. B273, 128 (1991)

[19] I.P. Lokhtin and A.M. Snigirev, Phys. At. Nucl. 60, 295 (1997); Z. Phys C73, 315 (1997)

[20] K.J. Eskola, K. Kajantie and P.V. Ruuskanen, Phys. Lett. B332 (1994) 191; Eur. Phys. J. C1 (1998) 627; K.J. Eskola, Prog. Theor. Phys. Suppl. 129, 1 (1997); Comments Nucl. Part. Phys. 22, 185 (1998); K.J. Eskola and K. Tuominen, Phys. Lett. B489, 329 (2000); K.J. Eskola, K. Kajantie, P.V. Ruuskanen and K. Tuominen, Nucl. Phys. B 570, 379 (2000)

[21] M. Bedjidian et al., “Heavy Ion Physics Programme in CMS”, CERN CMS Note 2000/060

[22] CMS Collaboration Technical Proposal, CERN/LHCC 94-38, 1994

[23] M. Gyulassy and M. Plümer, Phys. Lett. B243, 432 (1990)

[24] I.P. Lokhtin and A.M. Snigirev, Eur. Phys. J. C16, 527 (2000)

[25] M. Plümer, M. Gyulassy and X.-N. Wang, Nucl. Phys. A590, 511 (1995)

[26] I.P. Lokhtin, L.I. Sarycheva, and A.M. Snigirev, Phys. At. Nucl. 62, 1258 (1999)

[27] X.-N. Wang, Z. Huang and I. Sarcevic, Phys. Rev. Lett. 231, 77 (1996); X.-N. Wang and Z. Huang, Phys. Rev. C 55, 3047 (1997)

[28] V. Kartvelishvili, R. Kvatadze and R. Shanidze, Phys. Lett. B356, 589 (1995)

[29] E. Shuryak, Phys. Rev. 55, 961 (1997)

[30] B. Kampfer, O.P. Pavlenko and K. Gallmeister, Phys. Lett. B 419, 412 (1998)

[31] Z. Lin, R. Vogt and X.-N. Wang, Phys. Rev. C 57, 899 (1998); Z. Lin and R. Vogt, Nucl. Phys. B 544, 339 (1999)

[32] I.P. Lokhtin et al., “Jet Physics in CMS Heavy Ion Programme”, CERN CMS Note 1999/016

[33] ALICE Collaboration Technical Proposal, CERN/LHCC 95-71, 1995

[34] M.G. Mustafa, D. Pal, D.K. Srivastava and M. Thoma, Phys. Lett. B428, 234 (1998)

[35] J.F. Gunion and G. Bertch, Phys. Rev. D25, 746 (1982)

[36] J.D. Bjorken, Phys. Rev. D27, 140 (1983)

[37] M. Bedjidian, V. Karvelishvili and R. Kvatadze, “Study of high-mass dimuon production in Pb+Pb collisions with CMS”, CERN CMS Note 1999/017

[38] D.E. Groom et al., “Review of particle physics”, Eur. Phys. J C15 (2000) 1

[39] E. Norrbin, T. Sjöstrand, Eur. Phys. J. C 17, 137 (2000)

[40] M. Bedjidian, “Muon pairs detection with heavy ion beams in CMS”, CERN CMS Note 1999/052

[41] T. Sjöstrand. Comput. Phys. Commun. 82, 74 (1994)

[42] R. Vogt, Heavy Ion Phys. 9, 339 (1999)

[43] C.W. deJager, H. deVries and C. deVries, Atomic Data and Nuclear Data Tables 14, 485 (1974)

[44] K.J. Eskola, V.J. Kolhinen and C.A. Salgado, Eur. Phys. J. C9, 61 (1999)

[45] M. Bedjidian, O.L. Kodolova and S.V. Petrouchanko, “Dimuon reconstruction in heavy ion collisions using a detailed description of CMS geometry”, CERN CMS Note 1999/004

[46] E.L. Berger, B.W. Harris, D.E. Kaplan, Z. Sullivan, T.M.P. Tait and C.E.M. Wagner, hep-ph/0012001

[47] R.L. Thews, M. Schroedter and J. Rafelski, hep-ph/0007323

[48] P. Braun-Munzinger and K. Redlich, E. Phys. J. C16, 519 (2000)

[49] C.M. Ko, X.-N. Wang, and X.-F. Zhang, nucl-th/9808032.